Calculation for $l=2$ at 1.2 ev gives $Q_2=0.3\times10^{-16}$ cm^2 and a phase shift consistent with the angular distribution data. It is larger by a factor 4 than the best fit to the angular distribution obtained by Holtsmark[5] which has been used in Fig. 1. However, the higher value gives a better fit to the total cross section.

The cross section in the neighborhood of room temperature and below is strongly increased by the tail of the polarization force. If this tail is truncated by the presence of neighboring atoms, then the cross section will be reduced. The effect is strongest at zero energy, where the cross section (in units of 10^{-16} cm^2) is reduced from 7.5 to 6 for a cutoff at $r=60$, to 3 at $r=40$, and to 1 at $r=25$. This effect may explain the small value observed by Whalin who made measurements at 1 atmosphere but not that of Phelps, Fundingsland, and Brown which was made at a pressure of 1 mm of Hg.

We have applied the same method to predicting the eigenvalues of potassium using $p=8.5$.[12] Essentially the same potential fits the eigenvalues for $4s$, $6s$, $8s$, and $10s$. (The exchange force magnitude required is $\sim5\%$ larger for $4s$ than the others.) This establishes the validity of the static potential. The result is insensitive to the shape of polarization and exchange forces inside the atom because of the dominance of the Coulomb field. As in argon, a weaker ($\sim25\%$) exchange force was required for $l=1$ ($6p$) than for $l=0$ ($6s$).

ACKNOWLEDGMENTS

Much help has been received from H. Bethe, A. Kantrowitz, P. Hammerling, and F. Fusco.

[12] R. M. Sternheimer, Phys. Rev. **96**, 951 (1954).

PHYSICAL REVIEW VOLUME 116, NUMBER 4 NOVEMBER 15, 1959

Energy Dependence of Fast-Neutron Activation Cross Sections*

A. E. JOHNSRUD,† M. G. SILBERT,‡ AND H. H. BARSCHALL
University of Wisconsin, Madison, Wisconsin

(Received May 1, 1959)

Fast-neutron capture cross sections of 24 nuclides ranging from $A=51$ to $A=197$ have been measured by an activation method, in the neutron energy region from 0.15 to 6.2 Mev. The neutron energy spreads were of the order of 0.1 Mev so that cross sections averaged over many energy levels of the compound nucleus were measured. Activities induced in samples by fast and thermal neutrons were compared. The relative neutron flux in the fast- and thermal-neutron activations was determined with a U^{235} fission counter. A knowledge of the energy dependence of the U^{235} fission cross section and of the thermal-neutron activation cross sections allows calculation of the fast-neutron activation cross sections.

I. INTRODUCTION

MEASUREMENTS of the cross section for the radiative capture of fast neutrons have furnished valuable information about nuclear structure such as the dependence of level spacing on excitation energy and on nucleon number, and the effects of closed shells and of even or odd numbers of protons and neutrons on level spacing. Several authors[1–3] have calculated fast-neutron capture cross sections averaged over resonances. Most recently Lane and Lynn,[4] and Rae, Margolis, and Troubetzkoy[5] have calculated the energy dependence of the capture cross sections of U^{235}, U^{238}, and Th^{232} for neutron energies below 1 Mev. These calculations gave cross sections in good agreement with observations. There are, however, not many other isotopes for which the energy dependence of the capture cross section has been measured over a wide energy range, and there are inconsistencies in the reported results. For these reasons the present experiments were undertaken to measure capture cross sections of intermediate and heavy nuclei averaged over many energy levels in the compound nucleus, for neutrons in the energy range from 0.15 to 6.2 Mev.

Three methods for measuring fast-neutron capture cross sections are currently widely used: (1) observations of induced radioactivities,[6,7] (2) observations of capture γ-rays,[8] and (3) sphere transmission experiments.[9]

* Work supported by the U. S. Atomic Energy Commission and by the Graduate School from funds supplied by the Wisconsin Alumni Research Foundation.

† Present address: Hughes Aircraft Company, Culver City, California.

‡ Present address: Los Alamos Scientific Laboratory, Los Alamos, New Mexico.

[1] Feshbach, Peaslee, and Weisskopf, Phys. Rev. **71**, 145 (1947).

[2] E. P. Wigner, Am. J. Phys. **17**, 99 (1949).

[3] B. Margolis, Phys. Rev. **88**, 327 (1952).

[4] A. M. Lane and J. E. Lynn, Proc. Phys. Soc. (London) **A70**, 557 (1957).

[5] Rae, Margolis, and Troubetzkoy, Phys. Rev. **112**, 492 (1958).

[6] Segrè, Greisen, Linenberger, and Miskel, Atomic Energy Commission Report MDDC-228, 1946 (unpublished).

[7] Hughes, Spatz, and Goldstein, Phys. Rev. **75**, 1781 (1949); D. J. Hughes and D. Sherman, Phys. Rev. **78**, 632 (1950); Hughes, Garth, and Levin, Phys. Rev. **91**, 1423 (1953).

[8] Diven, Hemmendinger, and Terrell, *Proceedings of the Second United Nations International Conference on the Peaceful Uses of Atomic Energy, 1958* (United Nations, Geneva, 1958), Paper UN-667.

[9] A. O. Hanson, Los Alamos Report LA-276, 1945 (unpublished).

Since the latter two methods require relatively large amounts of material, they are normally applied to the naturally occurring isotopic mixture, while the first method measures an isotopic cross section, even when an isotopic mixture is used. The isotopic cross section can be more readily obtained theoretically than the cross section for a mixture of isotopes, since the calculation of the latter requires the addition of several isotopic cross sections.

Previous measurements[10] of the energy dependence of fast-neutron capture cross sections which were carried out at this laboratory used the activation method to demonstrate the effect of resonances on the capture cross sections of light nuclei and to measure radiation widths of the observed levels. The present experiments use a similar method for observing cross sections averaged over resonances. Although this method has the advantage of measuring isotopic cross sections, it can be applied conveniently to only a restricted number of isotopes which, upon addition of a neutron, produce a readily observable activity.

In order to study the variation of the capture cross section with energy it is most convenient to use an accelerated-particle source. Both the activation method[10–15] and the observation of γ rays have been used with such sources. Since the sphere transmission method[16] can be most conveniently used with an isotropic source, photoneutron sources are best suited for such measurements. At isolated energies many activation measurements have also been performed with photoneutron sources.[17,18] The most extensive measurements of activation cross sections were carried out by Hughes and co-workers[7] who used fission neutrons which have an average energy of about 1 Mev.

II. APPARATUS AND PROCEDURE

A. Method

Fast-neutron activation cross sections were determined through observations of induced radioactivities according to the method developed by Segrè[6] and Hughes.[7] In order to avoid the necessity for an absolute determination of neutron and γ-ray counting efficiencies, the activities induced by fast neutrons were compared to the activity induced by thermal neutrons in the same sample. The fast and thermal neutron fluxes were compared with a U^{235} fission counter. A knowledge of the energy dependence of the U^{235} fission cross section and of the thermal-neutron activation cross section allows calculation of the fast-neutron activation cross section.

In the previous measurements[10] at this laboratory the neutron flux was monitored by observations of α-particles from the reaction $B^{10}(n,\alpha)$. For the calculations of the capture cross sections, the boron disintegration cross section measured at Los Alamos in 1944 and plotted in Adair's review article[19] were used. More recent measurements[20,21] have shown that this boron cross section was too high by a factor of about two. Consequently all capture cross sections reported in reference 10 should be reduced by the ratio of the boron disintegration cross section reported in reference 21 to that reported in reference 19, i.e., by a factor of the order of two.

B. Apparatus

The activities induced in the samples were detected with a scintillation counting system utilizing a NaI(Tl) crystal. Gamma rays or x-rays accompanying beta decay or isomeric transitions in the product nucleus were observed. In order to obtain the best signal-to-background ratio, only scintillation pulses in a pulse-height interval centered approximately on a prominent photopeak in the spectrum were counted.

Fissions were observed in a cylindrical ionization chamber which contained a 0.45-mg/cm^2 layer of U^{235} oxide deposited on a cylindrical platinum backing.[22] For the calculation of the activation cross section a U^{235} fission cross section of 584 barns[23] was used for thermal neutrons, while for fast neutrons the values given by Allen and Henkel[24] were employed.

Samples to be activated were cylindrical rings, 2.5 cm long, 3.2 cm inside diameter, and 0.04 to 0.64 cm thick. The metallic samples were cast, machined, or rolled from sheet into the appropriate shape. The samples in powder form were packed into polyethylene or Teflon containers. In Table I the nuclides on which measurements were carried out are listed in the first column. These nuclides were chosen because of the convenient half-lives of the induced activities, the

[10] R. L. Henkel and H. H. Barschall, Phys. Rev. **80**, 145 (1950).
[11] A. T. G. Ferguson and E. B. Paul, J. Nuclear Energy **A10**, 19 (1959).
[12] H. C. Martin and R. F. Taschek, Phys. Rev. **89**, 1302 (1953).
[13] S. J. Bame and R. L. Cubitt, Phys. Rev. **113**, 256 (1959).
[14] Pasechnik, Barchuk, Totsky, Strizhak, Korolev, Gofman, and Lovchikova, *Proceedings of the Second United Nations International Conference on the Peaceful Uses of Atomic Energy, 1958* (United Nations, Geneva, 1958), Paper UN-2030.
[15] Leipunsky, Kazachkovsky, Artyukov, Baryshnikov, Galkov, Stavissky, Stumbur, and Sherman, *Proceedings of the Second United Nations International Conference on the Peaceful Uses of Atomic Energy, 1958* (United Nations, Geneva, 1958), Paper UN-2219.
[16] T. S. Belanova, J. Exptl. Theoret. Phys. U.S.S.R. **34**, 574 (1958) [translation: Soviet Phys. JETP **7**, 397 (1958)].
[17] L. E. Beghian and H. H. Halban, Nature **163**, 366 (1949); V. Hummel and B. Hammermesh, Phys. Rev. **82**, 67 (1951); Macklin, Lazar, and Lyon, Phys. Rev. **107**, 504 (1957); Booth, Ball, and MacGregor, Phys. Rev. **112**, 226 (1958).
[18] W. S. Lyon and R. L. Macklin, Phys. Rev. **114**, 1619 (1959).
[19] R. K. Adair, Revs. Modern Phys. **22**, 249 (1950).
[20] Petree, Johnson, and Miller, Phys. Rev. **83**, 1148 (1951).
[21] H. Bichsel and T. W. Bonner, Phys. Rev. **108**, 1025 (1957).
[22] The authors are indebted to Mr. J. Povelites and Dr. B. C. Diven of the Los Alamos Scientific Laboratory for the preparation of the U^{235} foil.
[23] D. J. Hughes and R. B. Schwartz, *Neutron Cross Sections*, Brookhaven National Laboratory Report BNL-325, (U. S. Government Printing Office, Washington, D. C., 1958), second edition.
[24] W. D. Allen and R. L. Henkel, *Progress in Nuclear Energy* (Pergamon Press, New York, 1958), Ser. I, Vol. II.

TABLE I. Information concerning the nuclides studied.

Nuclide	Half-life	Sample form	Thermal activation cross section (barns)	Standard error in thermal activation	γ- or x-ray peaks (kev)	Counting region (kev)	Ground-state spin and parity	Levels (Mev)
V^{51}	3.77 min	$V(p)$	4.5±0.9	±7%	230, 1450	180–∞	$7/2^-$	0.323 ($5/2^-$), 0.65, *0.928*, *1.614*, 1.819
Mn^{55}	2.58 hr	$MnO_2(p)$	13.3±0.2	7	850	740–1250	$5/2^-$	*0.128* ($7/2^-$), 0.59, *0.983*, *1.29*, *1.53*, 1.88, 2.20, 2.25, 2.27, 2.29, 2.31, 2.37, 2.40, 2.43, 2.56, others observed to 3.93
Co^{59} [a]	10.5 min	Co	16 ±3	7	59	42–83	$7/2^-$	*1.10* ($5/2^-$), *1.29* ($3/2^-$), *1.8*, *3.1*
Cu^{65}	5.1 min	Cu	1.8±0.4	7		50–420	$3/2^-$	0.770, 0.82 ($1/2^-$), *1.11*, 1.48, 1.62, 1.73, 2.09, 2.11, 2.21, 2.28, 2.33, 2.40, 2.53, 2.59, 2.65, 2.75, 2.84, 2.86, 2.89, 2.98, 3.04, 3.08
Ga^{71}	14.2 hr	$Ga(t)$	4.0±0.7	7	834	700–1000	$3/2^-$	0.513, 1.48, two additional states observed between 0.513 and 1.48
As^{75}	26.7 hr	$As(p)$	5.4±1.0	8	550	480–660	$3/2^-$	0.199, 0.265, 0.280, 0.305, 0.402 ($3/2^+$), 0.477, 0.572, 0.628, 0.78, *0.814*, *1.25*, *1.63*
Br^{79} [a]	18.0 min	$PbBr(t)$	8.5±1.4	7	85	46–122	$3/2^-$	0.217, 0.261, 0.307, 0.398, 0.606, 0.833
Br^{79} [a]	4.5 hr	$PbBr(t)$	2.9±0.5	10	85	46–122	$3/2^-$	
Br^{81}	35.9 hr	$PbBr(t)$	3.1±0.5	7	85	46–122	$3/2^-$	0.278
Sr^{86} [a]	2.80 hr	$SrO(t)$	1.3±0.4	8	388	279–488	0^+	
Mo^{100}	14.6 min	Mo	0.2±0.05	11		400–∞	0^+	0.53 (2^+)
Ag^{107}	2.3 min	Ag	45 ±4	7		50–420	$1/2^-$	0.093 ($7/2^+$), 0.324 ($3/2^-$), 0.423 ($5/2^-$), 0.939, 1.28
In^{115} [a]	54 min	In	155 ±10	7	137, 400, 800, 1090, 1300	100–∞	$9/2^+$	0.335 ($1/2^-$), *0.595* ($5/2^-$), 0.825 ($3/2^-$), 0.858 ($3/2^-$), *0.935* ($7/2^+$), 1.08, 1.14, 1.29 ($11/2^+$), *1.42* ($9/2^+$), 1.60, 1.98
I^{127}	25.0 min	$I(p)$	5.6±0.3	7	450	300–600	$5/2^+$	*0.057* ($7/2^+$), *0.203* ($3/2^+$), 0.373, *0.38*, *0.42*, *0.62*, *0.64*, 0.724, *0.74*, 0.94, *1.02*, *1.22*, *1.38*
Ba^{138}	85 min	Ba	0.5±0.1	8	160	75–235	0^+	1.43 (2^+), 1.89, 2.21, 2.30, 2.44 (3), 2.63, 3.34
La^{139}	40.2 hr	$La_2O_3(t)$	8.2±0.8	7	815, 1596	694–1750	$7/2^+$	0.165 ($5/2^+$), 1.5
Pr^{141}	19.2 hr	$Pr_6O_{11}(t)$	10 ±3	7		510–798	$5/2^+$	0.142 ($7/2^+$), 1.30 ($5/2^+$)
Nd^{148}	2.0 hr	$Nd_2O_3(t)$	3.7±1.2	12	118	67–163	0^+	0.300 (2^+)
Nd^{150}	12.0 min	$Nd_2O_3(t)$	3.0±1.5[b]	15	118	67–163	0^+	0.131 (2^+)
Eu^{151} [a]	9.2 hr	$Eu_2O_3(t)$	1400 ±300	7	122	75–161	$5/2^-$	0.022, 0.194, 0.304
Sm^{154}	24.0 min	$Sm_2O_3(p)$	5.5±1.1	10	105	70–150	0^+	0.082 (2^+)
Dy^{164} [a]	2.32 hr	$Dy_2O_3(p)$	2100 ±300	7	45	25–65	0^+	0.073 (2^+)
Ho^{165} [a]	27.3 hr	$Ho_2O_3(t)$	60 ±12	7	52	32–73	$7/2^-$	0.095 ($9/2^-$), 0.205 ($11/2^-$), 0.361, 0.52
W^{186}	24.0 hr	$W(p)$	34 ±7	7	72, 134, 480, 686	30–∞	0^+	0.123 (2^+)
Au^{197}	2.70 day	Au	99 ±2.0[b]	7	412	337–487	$3/2^+$	0.077 ($1/2^+$), 0.268 ($3/2^+$), *0.279* ($5/2^+$), *0.409*, ($11/2^-$), *0.548* ($7/2^+$), *1.22*, *1.68*, *2.2*, *2.6*, 3.0

[a] Cross section to one of two possible states.
[b] Thermal absorption cross section.

large fraction of decays which yielded γ rays or x-rays, and the availability of samples of high purity and in suitable form. Those marked with a [superscript a] are the nuclides for which the measured cross section is for capture to one of two possible states of the product nucleus. In the second column the half-lives of the induced activities which were studied in the present experiments are given as quoted in the review article by Strominger *et al.*[25] The chemical form of the samples is shown in column 3. (t) indicates that the sample was enclosed in 0.4-mm thick Teflon sheet, (p) that it was enclosed in 0.4-mm thick polyethylene sheet. The thermal-neutron activation cross sections (in barns) on which the present measurements are based are given in the fourth column. These values are taken from the compilation by Hughes *et al.*,[23] except the value for Au^{197} which is the result given by Gould *et al.*[26] The cross sections are for neutrons with a velocity of 2200 m/sec, except for Eu^{151} and Dy^{164} for which the only available activation cross sections are for pile neutrons. For Nd^{150}, the thermal activation cross section has not been determined so that the thermal absorption cross section is quoted. Since the thermal absorption cross section of Au^{197} is known much more accurately than the thermal activation cross section, the former has been used in the calculations. The fifth column gives the standard rms error in the present measurements of thermal neutron activation. This error combined with the uncertainty in the thermal activation cross section (column 4) determines the

[25] Strominger, Hollander, and Seaborg, Revs. Modern Phys. **30**, 585 (1958).

[26] Gould, Taylor, and Havens, Phys. Rev. **100**, 1248 (1955).

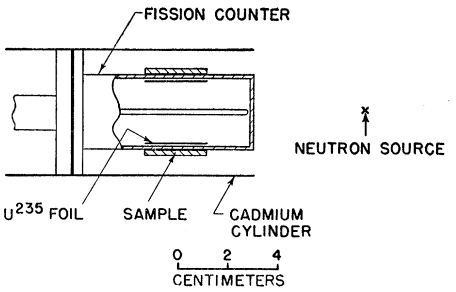

FIG. 1. Experimental arrangement for fast-neutron activations. The neutron source was the target of an electrostatic accelerator.

uncertainty in the normalization of the fast-neutron cross sections.

As a preliminary step the samples were activated by neutron bombardment and the scintillation spectra studied with a 20-channel pulse-height analyzer. The desired activity was identified both by γ- or x-ray energy and by half-life, and a suitable region of the spectrum for counting was chosen.

Columns 6 and 7 refer to the scintillation counting used to measure sample activity. The γ- or x-ray photopeaks which were observed in the scintillation spectrum, within the counting region indicated in column 7, are listed in column 6. The samples for which no peaks are listed are those for which the peaks were not resolved. The γ- and x-ray energies are those quoted in reference 25 and by McGowan and Stelson.[27] Column 8 gives the ground-state spin and parity of each target nucleus, as quoted by Strominger *et al.*[25] In column 9 are listed the known levels of the target nuclei, because of their importance to the energy dependence of the capture cross section. The position, spin, and parity of levels are taken from Strominger *et al.*,[25] Nuclear Data Cards and Nuclear Data Sheets.[28] Energies of levels which have been observed in inelastic scattering of neutrons are given in italics.

C. Procedure

1. Fast-Neutron Activations

Neutrons were produced in the energy region from 0.15 to 0.60 Mev by the Li(p,n) reaction, in the energy region from 0.60 to 2.5 Mev by the T(p,n) reaction, and in the energy region from 2.6 to 6.2 Mev by the D(d,n) reaction. Protons or deuterons were accelerated with an electrostatic generator. The Li target was metallic and of such thickness as to produce a neutron energy spread of about 50 kev. Gas targets of deuterium and tritium were used. All of the measurements with D(d,n) neutrons and some of the measurements with T(p,n) neutrons were carried out with a double-foil gas target, similar to that described by Nobles.[29] The energy spread of the T(p,n) neutrons, using this target, was about 170 kev, that of the D(d,n) neutrons, 380 kev. For the measurements on V, Mn, Cu, As, Mo, Ag, In, I, Ba, Sm, Dy, W, and Au a single-foil tritium target introduced an energy spread of about 80 kev. To simplify the figures only the larger energy spreads are shown for the T(p,n) neutrons.

The experimental arrangement for the fast-neutron activation is shown in Fig. 1. Each sample was fitted around the fission counter and the combination was placed coaxially with the proton or deuteron beam so that the distance from the center of the sample to the center of the neutron source was 8 cm. In this position, the relative neutron flux measured by the fission counter was nearly the same as that at the sample. A correction was applied for the difference in neutron flux at the sample and at the fission counter, caused by the difference in angle subtended at, and distance from the neutron source. To reduce the effect of room-scattered neutrons the sample and fission counter were enclosed by a 0.8-mm thick cylindrical Cd shield open at both ends.

The effect of room-scattered background neutrons was estimated by repeating activations at distances greater than normal from the neutron source and assuming that the direct neutron flux varied inversely with the square of the distance while the background neutron flux was constant. The effect of room-scattered background neutrons was always less than 8%, and at most energies less than 3%. When the D(d,n) reaction was used, activations were repeated with hydrogen replacing deuterium in the gas target so that the effect of background neutrons from deuteron reactions with nuclei other than deuterium in the target could be determined. The effect of these background neutrons became serious at the higher deuteron energies and was about 12% and 37% at the two highest deuteron energies, 2.4 and 3.2 Mev, corresponding to neutron energies of 5.5 and 6.2 Mev. The figures for the magnitude of the neutron background effect take into account the increase in both the sample activity and the fission counting rate and represent the correction that must be applied in the calculation of the cross sections.

A leaky-capacitor current integrator[30] was employed during the activations of samples with short-lived activities to compensate for fluctuations in the accelerator beam current. The beam current was collected on a capacitor which was shunted by a variable resistance in series with a sensitive galvanometer. The time constant of this combination was chosen to match the decay constant of the activity. The galvanometer current was then a measure of the sample activity.

Only a limited number of nuclides was investigated above 2.5 Mev because of low sample activity. In

[27] F. K. McGowan and P. H. Stelson, Phys. Rev. **107**, 1674 (1957).

[28] Nuclear Data Cards and Nuclear Data Sheets (National Academy of Sciences, National Research Council, Washington, D. C.).

[29] R. Nobles, Rev. Sci. Instr. **28**, 962 (1957).

[30] S. C. Snowdon, Phys. Rev. **78**, 299 (1950).

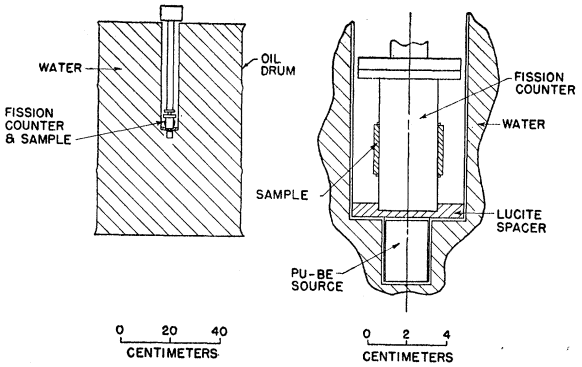

FIG. 2. Experimental arrangement for thermal-neutron activations.

addition, neutron-induced reactions, other than radiative capture, lead to the production of radioactive nuclei in some of the samples at the higher neutron energies. Extraneous activities induced were noticed as deviations from previously determined half-lives.

2. *Thermal-Neutron Activations*

Thermal neutrons were produced by slowing down neutrons from a Pu-Be source in water (Fig. 2). Thermal-neutron activations were carried out by placing the sample and fission counter in a well-defined position near the Pu-Be source, in the same position relative to each other as during fast-neutron activations. Thermal-neutron activations were repeated with a Cd shield enclosing the fission counter and sample, and the effect of epi-Cd neutrons was subtracted.

Although the samples depressed the thermal neutron flux, activations of a thin Ag probe showed that the flux was quite uniform along the samples. A small correction was applied for the difference between the flux at the inner surface where the fission foil was located, and the average of the flux at the inner and outer surfaces of the samples. The uncertainty in this correction for flux depression is included in the error in the thermal-neutron activation quoted in Table I.

The "thermal" neutron spectrum is approximately Maxwellian below the Cd cutoff. The thermal-neutron activation cross sections of the nuclides studied and the thermal-neutron fission cross section of U^{235} used in the calculations are for neutrons with an energy of 0.025 ev, with the exceptions noted in Sec. II-B. Rigorously, the cross sections employed in the calculations should be cross sections integrated over the neutron spectrum. The energy dependence of the activation cross sections, however, is similar enough to that of the U^{235} fission cross section in the energy region below the Cd cutoff, that, based on the observed Cd ratios and the assumed neutron spectrum, the error in the normalization of the fast-neutron capture cross sections caused by the use of 0.025-ev cross sections is estimated to be less than 3%.

III. RESULTS

The isotopic capture cross sections measured in the present experiment are plotted as a function of neutron energy in Figs. 3, 4, and 5. The triangles at the bottom of the figures represent neutron energy spreads. The arrows indicate the positions of known levels in the target nuclei (Table I); cross-hatched areas indicate many closely-spaced levels.

The error bars indicate the rms standard errors in the relative values of the cross sections. In addition, there is an uncertainty in the absolute value caused by the uncertainties in the measured thermal-neutron activation (Table I, column 5) and the uncertainty in the assumed thermal-neutron activation cross section (Table I, column 4). The errors in the absolute values of the capture cross sections have not been included in the error bars, because the cross sections can be readily adjusted as more accurate values of the thermal activation cross sections become available.

The capture cross section of Sr^{86} (to the 2.8-hr state) has been measured only below 0.39 Mev in the present experiment. Neutrons with energies greater than 0.39 Mev can be inelastically scattered from the stable isotope Sr^{87}, producing the state Sr^{87m}, the decay of which was observed to measure the capture cross section of Sr^{86}. Therefore, the activity produced in the Sr sample by such neutrons was the sum of that produced by capture and by inelastic scattering. The resulting apparent cross section increases by about a factor of 10 between 0.40 and 2.5 Mev.

Results obtained by other investigators are shown on the same figures for comparison. Cross sections based on the capture cross section of I^{127} have been adjusted to the present I^{127} cross section.

The figures show data obtained by the following investigators who used accelerated-particle neutron sources: Pasechnik *et al.*,[14] who compared fast-neutron activation cross sections to the activation cross section of I^{127}; Diven,[8] who measured capture-γ rays; Bame and Cubitt,[13] who measured activation cross sections by absolute β counting; and Ferguson and Paul,[11] who measured the activation cross section of Au^{197} by absolute γ counting.

The following investigators used photoneutron sources: Belanova,[16] who used the sphere-transmission method; Lyon and Macklin,[18] who measured activation cross sections by absolute γ counting; and Leipunsky *et al.*,[15] who used both accelerated-particle neutron sources and photoneutron sources to compare fast-neutron activation cross sections to the I^{127} cross section.

The results of Martin and Taschek[12] for I^{127} have not been plotted since they have been superseded by the measurements of Bame and Cubitt.[13]

The agreement between the present results and those of other investigators is fairly good. The present results for I^{127} lie about 20% below the results of Bame

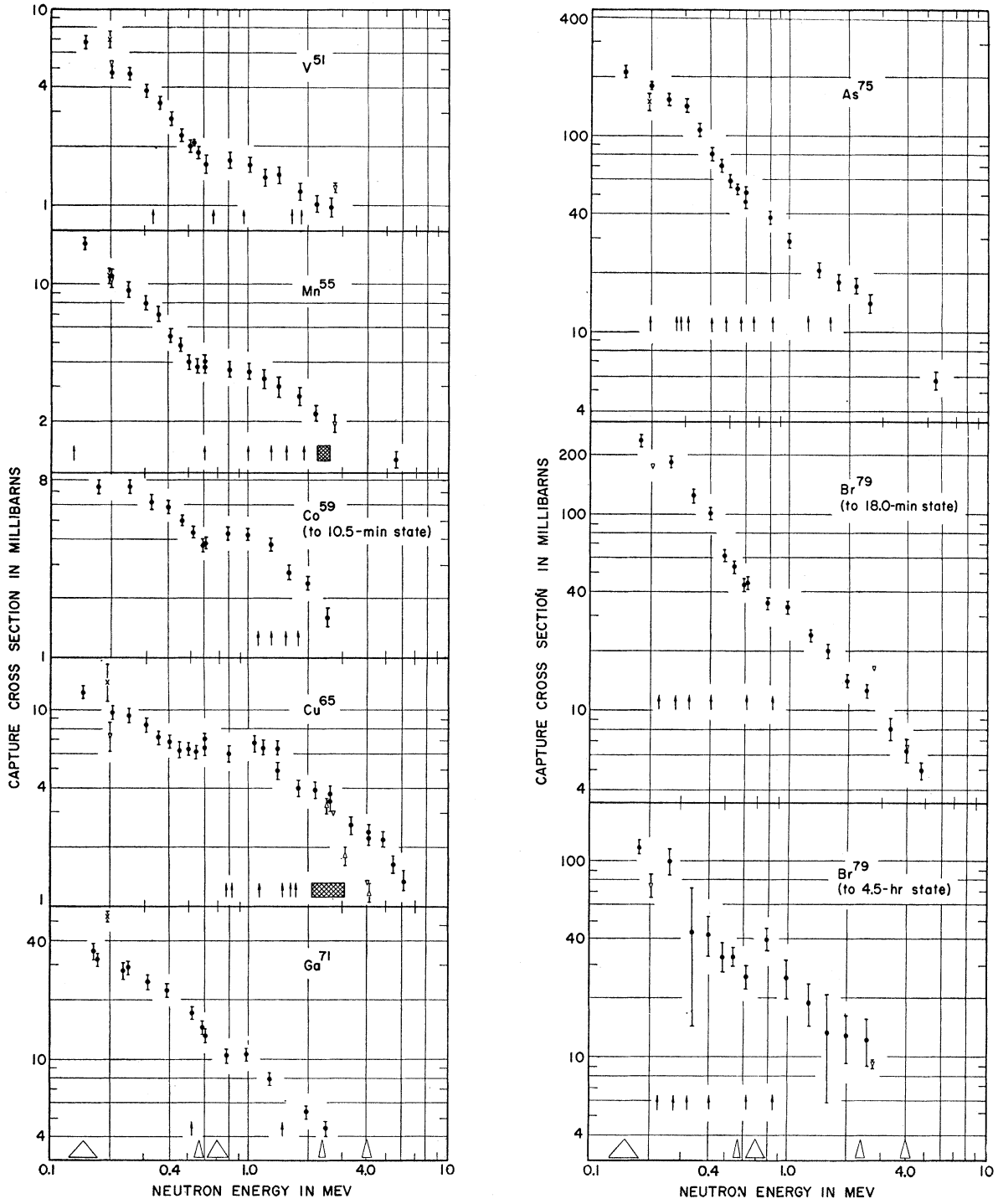

FIG. 3. Capture cross sections of V^{51}, Mn^{55}, Co^{59}, Cu^{65}, Ga^{71}, As^{75}, and Br^{79} as a function of neutron energy. Closed circles ● represent present data. For comparison the following results have also been plotted: △, reference 14; ▽, reference 15; ×, reference 18. Arrows indicate the positions of known levels in the target nuclei (Table I); cross-hatched areas indicate several closely spaced levels. Triangles at the bottom of the figure show neutron energy spreads with the exceptions noted in Sec. II-C-1 of the text. The indicated errors are the rms standard errors in the relative values of the cross sections and do not include errors in the absolute values (Sec. III of the text).

and Cubitt. In addition, the capture cross sections measured by Pasechnik and Leipunsky which have been adjusted to the present values of the I^{127} capture cross section appear to be generally lower than the

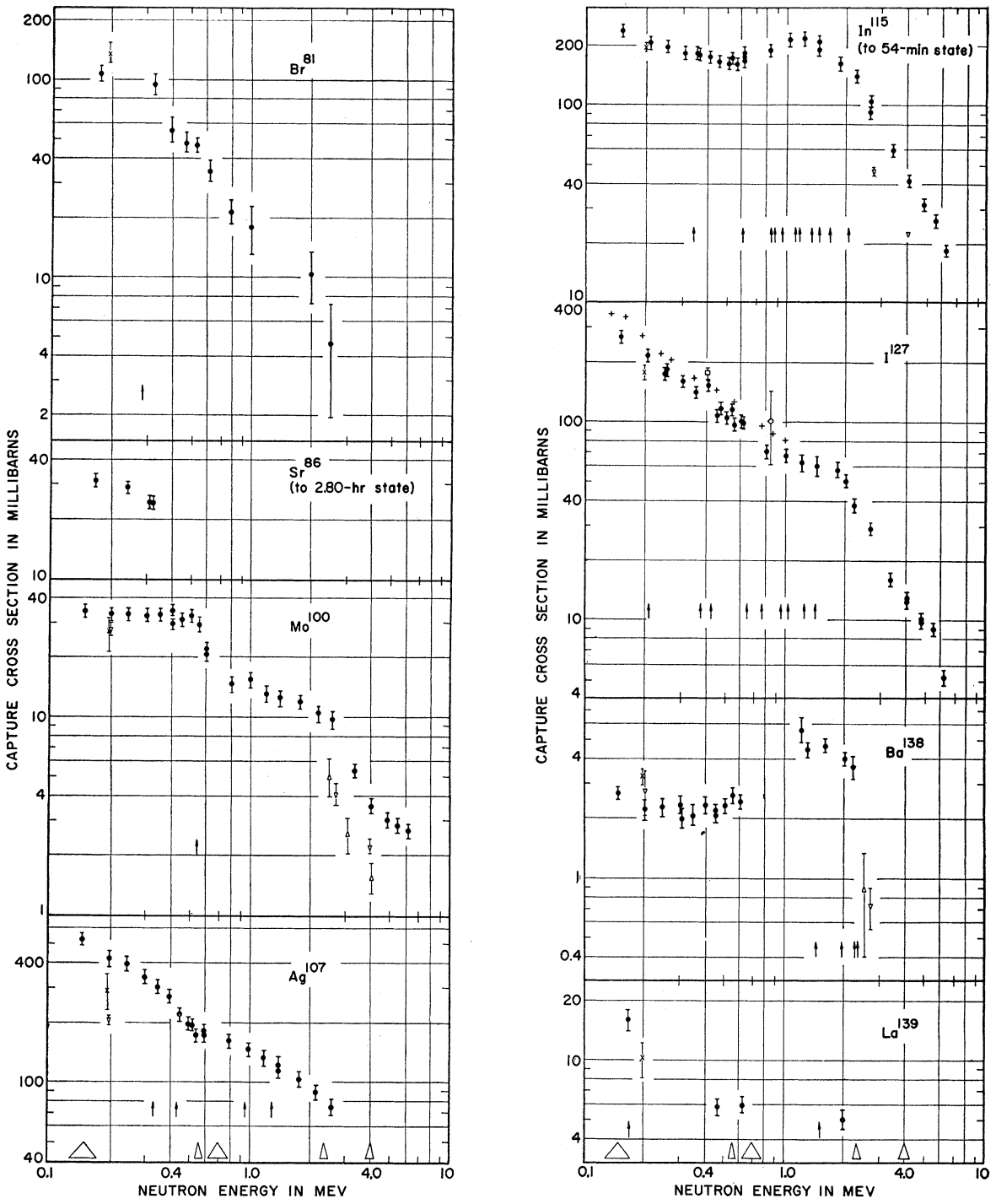

FIG. 4. Capture cross sections of Br^{81}, Sr^{86}, Mo^{100}, Ag^{107}, In^{115}, I^{127}, Ba^{138}, and La^{139} as a function of energy. Closed circles represent present data. For comparison the following results have also been plotted: △, reference 14; ▽, reference 15; □, reference 8; ◇, reference 16; ×, reference 18; +, reference 13.

present values, for the nuclides for which comparisons are possible. This suggests that the present results for I^{127} are low. Since the present results for Au^{197} are in good agreement with the work of Diven[8] and of Ferguson and Paul,[11] a possible cause of the disagreements in the I cross section could be that the thermal activation cross section of I which was used in the present determination is low. A large number of

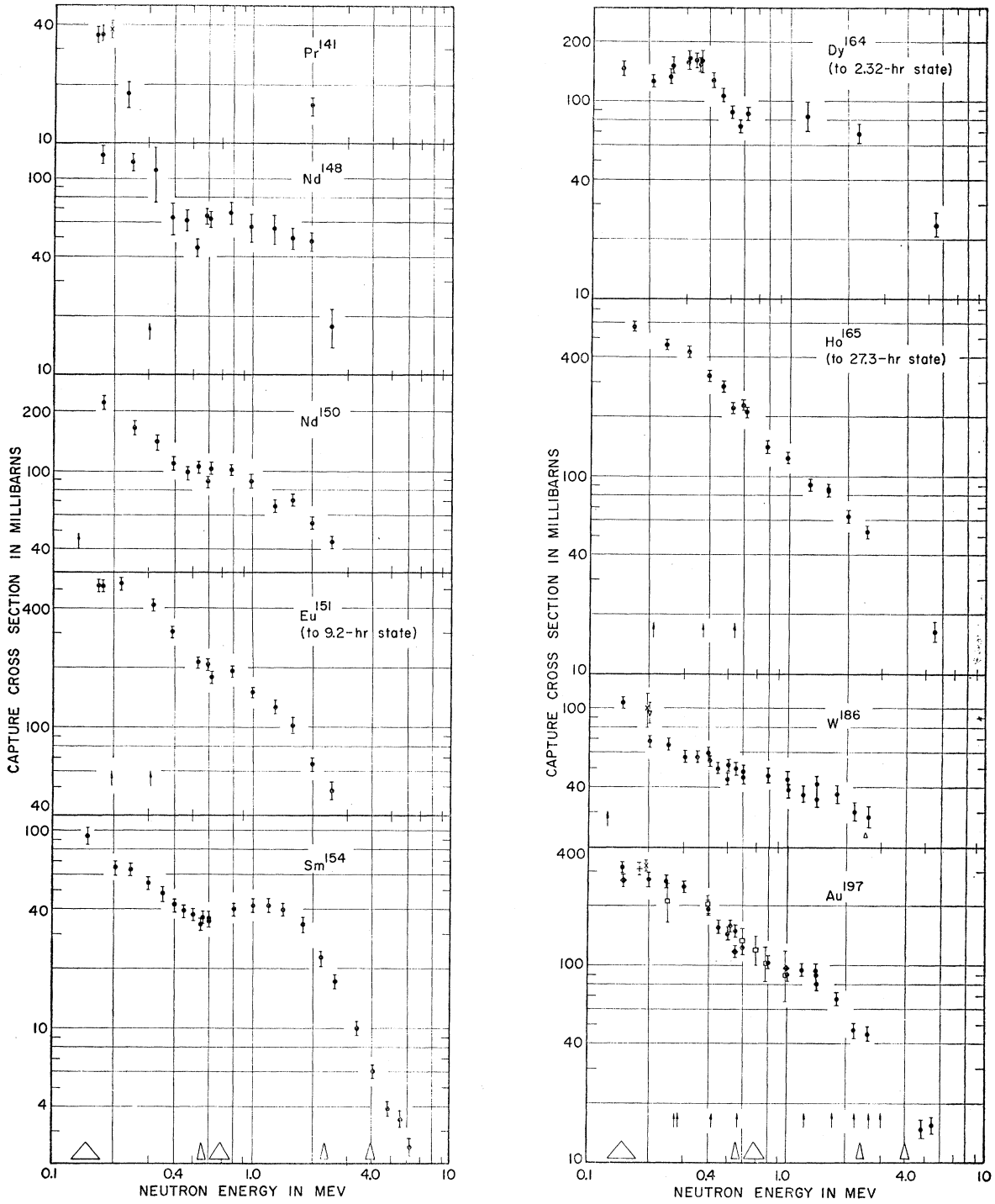

FIG. 5. Capture cross sections of Pr^{141}, Nd^{148}, Nd^{150}, Eu^{151}, Sm^{154}, Dy^{164}, Ho^{165}, W^{186}, and Au^{197} as a function of energy. Closed circles represent present data. For comparison the following results have also been plotted: △, reference 14; ▽, reference 15; □, reference 8; ×, reference 18; +, reference 13; closed diamonds, reference 11.

comparison data are available for I and Au because these elements have only one naturally-occurring isotope, so that the activation cross sections can be directly compared with cross sections measured by the capture-γ and sphere-transmission methods.

The present results agree fairly well with the measurements of Hughes *et al.*[7] with fission neutrons. The latter results are not shown in the figures, since they are not directly comparable with present measurements. The magnitude of the largest disagreement is about

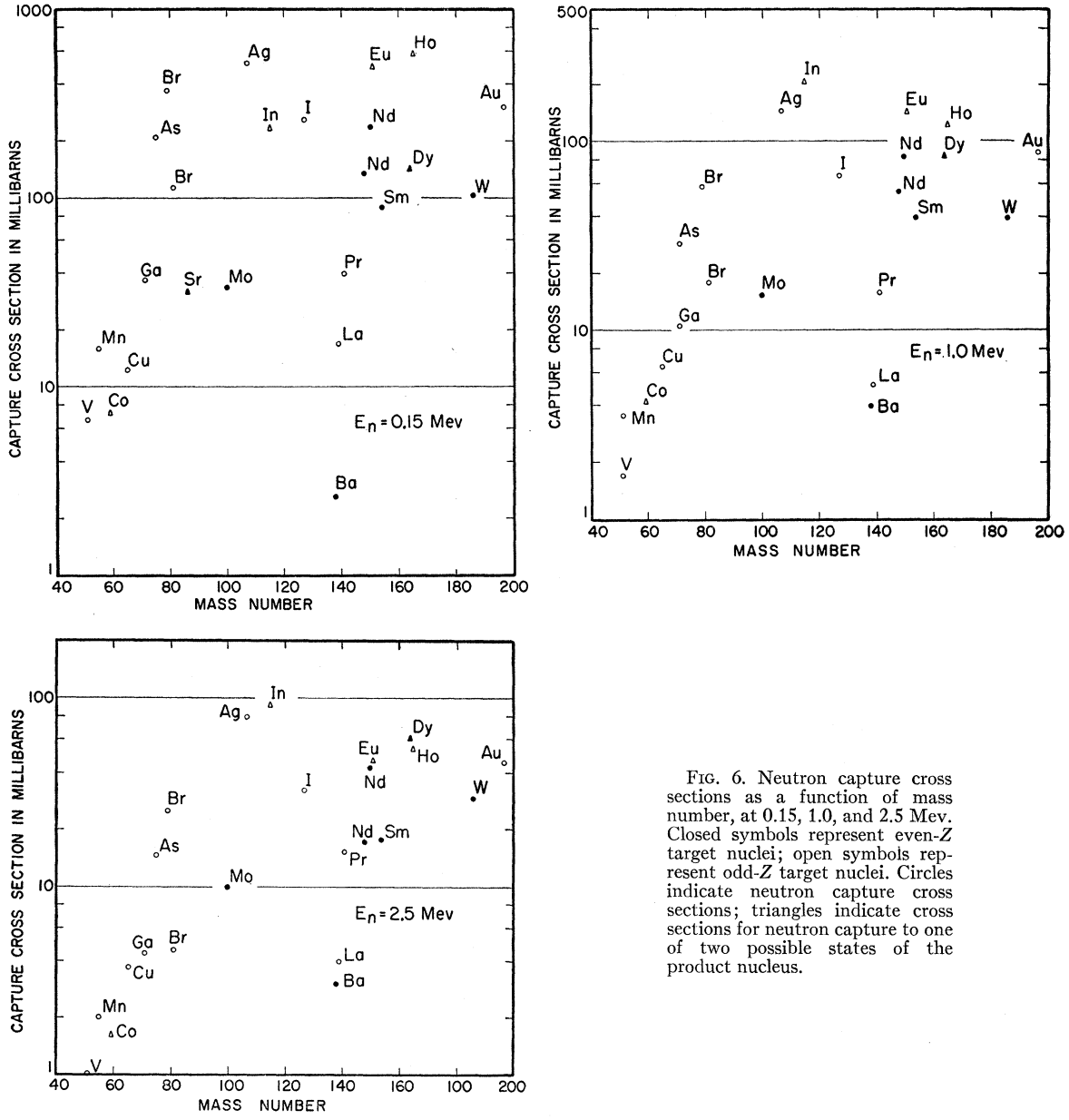

FIG. 6. Neutron capture cross sections as a function of mass number, at 0.15, 1.0, and 2.5 Mev. Closed symbols represent even-Z target nuclei; open symbols represent odd-Z target nuclei. Circles indicate neutron capture cross sections; triangles indicate cross sections for neutron capture to one of two possible states of the product nucleus.

50% of the present values if an energy of 1 Mev is assumed for the fission neutron spectrum.

Corrections were applied to the data for the following effects: neutron background; difference in neutron flux at the U^{235} foil and at the sample; decay of activity during neutron bombardment, for the samples with half-lives long enough so that the leaky-condenser current integrator was not used; and mis-match between the time constant of the leaky-condenser current integrator and the decay constant of the sample.

IV. DISCUSSION

In Fig. 6 the capture cross sections measured in the present experiment have been plotted as a function of mass number, for neutrons with energies of 0.15, 1.0, and 2.5 Mev. The open symbols indicate odd-Z nuclei, the closed symbols indicate even-Z nuclei. Triangles indicate those cross sections which are for capture to one of two possible states of the product nucleus, and are lower limits to the values which might be compared to circles. The same general behavior found by other investigators can be seen in this figure: the capture cross sections increase with A up to approximately $A=100$, then are roughly constant except for closed shell and even- or odd-Z effects. A minimum is evident for the nuclides Ba^{138}, La^{139}, and Pr^{141}, which have 82 neutrons. The odd-Z nuclides have larger neutron capture cross sections than the even-Z nuclides,

in the cases for which a comparison between nuclides of nearly the same mass numbers is possible. The variation of the capture cross section with mass number can be largely attributed to the variation of compound nucleus level spacing with mass number.

Plots at the three energies do not differ greatly, except in the obvious general decrease in cross section as a function of energy. There is some tendency for the cross sections that are lowest, i.e., those for even-Z and magic neutron-number nuclei, to decrease more slowly with energy than the cross sections of other nuclei. It has been suggested by Weinberg and Wigner[31] that the effect of neutrons with angular momenta higher than $l=0$ is of greater importance for those nuclei for which the compound nucleus formed by the addition of a neutron has a low level-density. Therefore such nuclei would be expected to exhibit neutron capture cross sections which decrease less rapidly as a function of energy than the cross sections of nuclei in general. This behavior is also evident in Figs. 3, 4, and 5.

The capture cross sections as a function of neutron energy, presented in Figs. 3, 4, and 5, do not follow a systematic pattern in progressing to successively higher mass numbers, with the exception of the first four nuclides, V^{51} to Cu^{65}. In this sequence a plateau appears in the cross section between about 0.6 and 1.0 Mev. It becomes more pronounced as A increases from 51 to 65, is vestigial at $A=71$, and has disappeared at $A=75$. The cross sections of In^{115}, Ba^{138}, and Sm^{154} also begin to increase in this neutron energy region, and pass through maxima somewhat above 1 Mev.

The cross section for the capture of fast neutrons is expected to be inversely proportional to the energy at neutron energies high enough so that the neutron width is much larger than the radiation width, if the effect of only s-wave neutrons is considered and if the effect of inelastic scattering is neglected. At lower energies, where the radiation width is much larger than the neutron width, the cross section is expected to be inversely proportional to the square root of the energy. The transition point, where the radiation width and neutron width are equal, occurs near 1 kev for nuclei with $A\sim50$ and near 300 kev for nuclei with $A\sim240$. However, in the 0.1- to 1.0-Mev region the effect of neutrons with higher orbital angular momentum is appreciable. Lane and Lynn[4] and Rae *et al.*[5] found it necessary to include f-wave neutrons even below 1 Mev in their calculations of capture cross sections of heavy nuclei. The neutrons of higher angular momentum cause the capture cross section to decrease more slowly than $1/E$ and may even produce a maximum in the cross section. On the other hand, inelastic scattering contributes to the total level width as the incident neutron energy is raised above the energy of excited states of the target nucleus. In general, competition between inelastic-neutron and γ emission in the compound nucleus is sufficient to produce a monotonically decreasing capture cross section. In a target nucleus such as U^{238}, which exhibits a "rotational" spectrum, the level density may, however, decrease as a function of energy, at low excitation energies. The competition from inelastic scattering may then be so small that the neutrons of higher angular momentum produce a flat region or even a maximum in the capture cross section.[4] At energies above a few Mev the increase in level density in the target nucleus is sufficient to produce monotonically decreasing capture cross sections.

The effect of competition between inelastic neutron scattering and γ emission is evident in the energy dependence of some of the capture cross sections. In these cases rapid decreases in the capture cross section can be correlated with the positions of known levels in the target nucleus. This effect can be observed above the 0.305-Mev level in As^{75}, the 0.261- and 0.398-Mev levels in Br^{79}, the 0.278-Mev level in Br^{81}, the 0.528-Mev level in Mo^{100}, and the 0.300-Mev level in Nd^{148}. The change from an increasing to a decreasing cross section observed in In^{115} and Ba^{138} may be correlated with the levels in these nuclei at 1.42 and 1.43 Mev, respectively.

An analysis of some of the present data and a discussion of the information obtainable from fitting the data with calculations based on the statistical theory of nuclear reactions[3,5] will be given in a paper by Mossin-Kotin, Margolis, and Troubetzkoy.[32]

[31] A. M. Weinberg and E. P. Wigner, *The Physical Theory of Neutron Chain Reactors* (The University of Chicago Press, Chicago, 1958).

[32] Mossin-Kotin, Margolis, and Troubetzkoy, following paper [Phys. Rev. **116**, 937 (1959)].